PARAMETRIC STUDY OF LAMINAR FREE CONVECTION IN HORIZONTAL ANNULUS WITH AND WITHOUT FINS ON THE INNER CYLINDER

Asst. Prof. Dr. Saad M. Saleh
Mechanical Engineering Department
University of Baghdad

Jasim Mohammed Mehdi
Mechanical Engineering Department
University of Baghdad

ABSTRACT

An experimental and numerical study has been carried out to investigate the heat transfer by natural convection in air-filled annulus between two horizontal isothermal concentric cylinders with and without annular fins under steady state conditions; the inner cylinder surface is maintained at a higher temperature and the outer cylinder surface at a lower one.

In the experimental study, the annulus inner surface is maintained at high temperature by applying uniform heat flux to the inner cylinder while the annulus outer surface is subjected to ambient temperature and maintained at low temperature. The experiments were curried out at a range of Rayleigh number (1.81×10^3 – 4.03×10^4) for case without fins and (1.08×10^3 – 2.94×10^4) for case with fins, at different diameter ratios (η = 2.0, 2.6 and 3.0). The results showed that: (1) increasing the diameter ratio(η) strongly increases the heat transfer rate, (2) increasing Rayleigh number increases the heat transfer rate for any η and (3) attaching annular fins to the inner cylinder surface of (No. of fins/cm) of 1.25 and (fin height/gap width) of 0.143, 0.186 and 0.286 reduced the mean Nusselt number ($\overline{Nu}$) within (16.3 - 29.7) percent of that for the case without fins at the same Rayleigh number. In the numerical study, only the case without fins was investigated. The buoyancy driven fluid flow resulting from the temperature difference between the cylinders, is assumed to be steady, laminar, two dimensional and symmetric about the vertical center-line. Only half of the domain needs to be modeled from symmetry considerations. Navier-Stokes and energy equations are expressed in vorticity-stream function form and discretized via finite difference method. The Rayleigh number (based on gap width) varied from $l0^2$ to $l0^5$ with the influence of diameter ratio obtained near a Rayleigh number of 10^4. Results for the local and mean Nusselt number, the contour maps of the streamlines and isotherms are presented, to show some of the flow and heat transfer characteristics. The results numerically obtained showed a good agreement with the present experimental data.

الخلاصة

أُجريتْ دراسة عملية ونظرية لاستقصاء انتقال الحرارة بالحمل الطبيعي خلال فجوة حلقية مملؤة هواء تقع بين اسطوانتين أفقيتين متحدتي المركز بثبوت درجة حرارة السطحين الداخلي و الخارجي للفجوة و بوجود و عدم وجود زعانف حلقية، تحت شروط حالة الاستقرار، وأن تكون الاسطوانة الداخلية ذات درجة حرارة أعلى من الخارجية.

في الدراسة العملية تم حفظ السطح الداخلي للفجوة بدرجة حرارة أعلى عن طريق تسليط فيض حراري منتظم على السطح الداخلي للاسطوانة الداخلية فيما حفظ السطح الخارجي للفجوة بدرجة حرارة أقل بتعريض الاسطوانة الخارجية الى درجة حرارة الجو. أجريت التجارب ضمن مدى لعدد رالي تراوح بين (1.81×10^3 – 4.03×10^4) للحالة بدون زعانف، و (1.08×10^3 – 2.94×10^4) للحالة بوجود زعانف،و عند نسبة أقطار(3.0 , 2.6 ,2.0). أظهرت النتائج بان زيادة نسبة الاقطار تزيد من معدل انتقال الحرارة بين الاسطوانتين، كذلك إنَّ الزيادة في عدد رالي تؤدي الى زيادة معدل انتقال الحرارة لاي نسبة أقطار، و إن اضافة زعانف حلقية الى الاسطوانة الداخلية بشكل تكميلي بمعدل 1.25 زعنفة لكل سنتمتر واحد و بنسبة (ارتفاع الزعنفة/ سمك الفجوة) 0.286 , 0.186 ,0.143 يقلل من رقم نسلت المعدل بحوالي (29.7% - 16.3%) مقارنة بالحالة بدون زعانف و لرقم رالي نفسه. تناولت الدراسة النظرية حل مسألة انتقال الحرارة بالحمل الحر خلال فجوة حلقية أفقية و للحالة بدون زعانف فقط ، إذ تم افتراض جريان المائع الناشيء عن قوى الطفو و نتيجة للفارق في درجة حرارة الاسطوانتين، هو جريان مستقر، طباقي ، ثنائي البعد و متناظر حول الخط المستقيم الشاقولي المار بالمركز. و نتيجة لاعتبارات التناظر فقط نصف واحد من نصفي الفجوة أخضع للدراسة. تم تمثيل معدلات نافير-ستوكس بالاضافة الى معادلة الطاقة بصيغة الدوامية- دالة الجريان و من ثم فُكت باستخدام طريقة الفروقات المحددة. و قد تم الحصول على نتائج مُثلت بمخططات دالة الجريان وخطوط تساوي درجة الحرارة، وتوزيع عدد نسلت الموضعي و المعدل خلال الفجوة ولأعداد رالي تتراوح بين 10^2الى 10^5 و نسب قطر خارجي إلى قطر داخلي(3.0 , 2.6 ,2.0) . بينت النتائج التأثير المهم للمتغيرات(رقم رالي و نسبة الاقطار)على عملية انتقال الحرارة خلال الفجوة و قد أظهرت النتائج المستحصلة عددياً توافقاً جيداً مع النتائج العملية.

KEYWORDS: Free Convection, Fins, Laminar, Horizontal Annulus.

INTRODUCTION

Natural convection in the annulus between two horizontal concentric cylinders has been investigated widely in the past owing to a number of practical applications associated with this geometry such as heat transfer and fluid flow in parabolic cylindrical solar collector, under-ground electrical transmission lines and pressurized water reactors. **Kuhen and Goldstein [1]** carried out an experimental and numerical investigation of natural convection heat transfer for air and water in concentric horizontal annuli for values of Rayleigh number up to 10^7. Their work was carried out for a diameter ratio equal to 2.6. In their experimental study, it was reported that the transition from laminar to turbulent flow occurs at Rayleigh number equal to 10^6. Later, **Hessami et al. [2]** studied experimentally the free convection in a horizontal annulus with a large diameter ratio of (11.4). The test fluids were air, glycerin and mercury. This study was unique as they clamed because there are no experimental details in the literature for $\eta > 8.1$. In addition, no experimental data exist for mercury. Recently **Nada [3]** conducted an experimental study of natural convection in horizontal and inclined annuli at Rayleigh number of ($5\times10^4 \le Ra_{Di} \le 5\times10^5$) for different diameter ratios (η=1.85, 2.5 and 3.85) and different inclination angle of the annulus ($\varphi = 0^\circ$, 30° and 60°). The results showed that increasing the annulus gap width strongly increases the heat transfer rate and the heat transfer rate slightly decreases with increasing the inclination of the annulus from the horizontal. Also, several numerical investigations of laminar natural convection in a concentric horizontal annulus have been conducted **[4–6]**. In these previous works, maximum transition time to attain steady state in underground electrical transmission lines, the

effects of variable properties on the laminar natural convection of gases in horizontal isothermal annulus and the effect of application constant heat flux on the inner cylinder as compared to an isothermal inner cylinder were studied.

An essential restriction in natural convection in annulus is the heat transfer limitation due to the fixed area of the inner and outer cylinders. One approach affecting heat transfer rate in annulus is to equip the surface of the inner cylinder with some annular fins. From a practical point of view, the existence of such fins is of interest due to the possibility of heat transfer augmentation in such geometry; but also heat transfer reduction is expected since existence of fins will resist the natural circulation inside the annulus. **Patankar and Chai [7]** studied the flow and heat transfer for an annulus with six radial fins attached to inner cylinder at ($Ra \leq 10^6$); for two different orientations; the first is when two fins of the six are vertical and the second is when two fins are horizontal. They observed that the orientation of the fins has no significant effect on mean Nusselt number prediction, while the blockage due to the presence of fins has a significant effect on the flow and temperature fields and therefore on heat transfer. Their results indicate that the mean Nusselt number decreases with increasing fin height. **Rahinam and Farhadi [8]** investigated the effect of radial fins on heat transfer by turbulent natural convection for an annulus with a number of radial fins ranged from 2 to 12 attached to inner cylinder. They examined two different orientations used by Patankar and Chai [7] to reveal the effect of fin height and fin orientation. The Rayleigh number considered in this study ranges from 10^6 to 10^9. Their results show that the higher fin height has a blocking effect on flow causing lower heat transfer rate. they concludes that there is a reduction of heat transfer rate in all of the orientations considered in this study as compared to the case of no fin at the same Rayleigh number.

The main aim of the present experimental investigation is to determine the effect of the annular fins, diameter ratio and Rayleigh number on mean Nusselt number prediction across the annulus. The numerical study objectives are to develop a mathematical model capable of predicting fluid flow and heat transfer in horizontal concentric annuli without fins using finite difference method for a range of Rayleigh numbers and diameter ratios.

NUMERICAL STUDY

Mathematical modeling

The governing equations for the natural convection in the annulus between horizontal concentric cylinders under steady-state conditions can be written as: [1]

$$\frac{1}{r}\frac{\partial}{\partial r}(ru)+\frac{1}{r}\frac{\partial v}{\partial \phi}=0 \quad \text{.....} \quad (1)$$

$$\rho_o\left[u\frac{\partial u}{\partial r}+\frac{v}{r}\frac{\partial u}{\partial \varphi}-\frac{v^2}{r}\right]=-\frac{\partial p}{\partial r}+\mu\left[\frac{\partial}{\partial r}\left(\frac{1}{r}\frac{\partial}{\partial r}(ru)\right)+\frac{1}{r^2}\frac{\partial^2 u}{\partial \phi^2}-\frac{2}{r^2}\frac{\partial v}{\partial \phi}\right]-g\rho_o\left[1-\beta(T-T_o)\right]\cos\phi \quad \text{.....} \quad (2)$$

$$\rho_o\left[ru\frac{\partial v}{\partial r}+v\frac{\partial v}{\partial \phi}+uv\right]=-\frac{\partial p}{\partial \phi}+\mu\left[r\frac{\partial}{\partial r}\left(\frac{1}{r}\frac{\partial}{\partial r}(rv)\right)+\right.$$

$$\frac{1}{r}\frac{\partial^2 v}{\partial\phi^2}+\frac{2}{r}\frac{\partial u}{\partial\phi}\Bigg]+g\rho_o r\left[1-\beta\left(T-T_o\right)\right]\sin\phi \quad \text{..... (3)}$$

$$u\frac{\partial T}{\partial r}+\frac{v}{r}\frac{\partial T}{\partial\varphi}=\alpha\left[\frac{1}{r}\frac{\partial}{\partial r}\left(\frac{\partial T}{\partial r}\right)+\frac{1}{r^2}\frac{\partial^2 T}{\partial\varphi^2}\right] \quad \text{..... (4)}$$

where the co-ordinate r is measured from the center of the system, and ϕ is measured clockwise from the upward vertical line; as shown in Fig.(1). The use of vorticity–streamfunction formulation can simplify the solution procedure. With the streamfunction, the velocity components u and v can be expressed as

$$u=\frac{1}{r}\frac{\partial\psi}{\partial\phi},\quad v=-\frac{\partial\psi}{\partial r}$$

Furthermore, by setting

$$R=\frac{r}{\delta}\qquad \Psi=\frac{\psi}{\alpha}\qquad \Omega=\frac{\delta^2}{\alpha}\omega\qquad \theta=\frac{T-T_o}{T_i-T_o}$$

where $\alpha=k/\rho c$ is the thermal diffusivity, δ is the gap between the cylinders and ω is the vorticity, Equations (1)–(4) can be simplified as

$$\nabla^2\Omega=\frac{1}{Pr}\left[U\frac{\partial\Omega}{\partial R}+\frac{V}{R}\frac{\partial\Omega}{\partial\phi}\right]+Ra\left[\frac{\cos\phi}{R}\frac{\partial\theta}{\partial\phi}+\sin\phi\frac{\partial\theta}{\partial R}\right] \text{..... (5)}$$

$$\nabla^2\Psi=-\Omega \quad \text{..... (6)}$$

$$U=\frac{1}{R}\frac{\partial\Psi}{\partial\phi},\quad V=-\frac{\partial\Psi}{\partial R} \quad \text{..... (7)}$$

$$\nabla^2\theta=U\frac{\partial\theta}{\partial R}+\frac{V}{R}\frac{\partial\theta}{\partial\phi} \quad \text{..... (8)}$$

∇ is Laplacian in polar coordinates and defined as; $\nabla^2=\frac{\partial^2}{\partial R^2}+\frac{1}{R}\frac{\partial}{\partial R}+\frac{1}{R^2}\frac{\partial^2}{\partial\phi^2}$

The dimensionless parameters appearing in the Equations (5)–(8) are the Prandtl number $Pr = \nu/\alpha$ and the Rayleigh number $Ra = g\beta(T_i-T_o)\delta^3/\alpha\nu$.

For the natural convection in an annulus between two concentric cylinders, the flow is symmetric with respect to the vertical centerline. Thus, half of the annulus can be taken as the computational domain, i.e. attention is restricted to ($0 < \phi < \pi$).

The boundary conditions on two impermeable isothermal walls are given by

$$\Psi=U=V=0\qquad \Omega=-\frac{\partial^2\Psi}{\partial R^2}\qquad \theta=1$$

on the inner cylinder and

$$\Psi = U = V = 0 \qquad \Omega = -\frac{\partial^2 \Psi}{\partial R^2} \qquad \theta = 0$$

on the outer cylinder. When half of the annulus is taken as the computational domain, the following symmetric condition is applied along two vertical lines of symmetry at $\phi = 0$ and $\phi = \pi$:

$$\Psi = U = V = 0 \qquad \Omega = 0 \qquad \frac{\partial \theta}{\partial \phi} = 0$$

The local and mean Nusselt number on inner cylinder surface is respectively expressed by the equations below: [4]

$$Nu = -\left.\frac{\partial \theta}{\partial R}\right|_{R=R_i} \quad \ldots\ldots\ldots\ldots\ldots\ldots\ldots\ldots\ldots\ldots \quad (9)$$

$$\overline{Nu} = \frac{1}{\pi}\int_0^{\pi} Nu.d\phi \quad \ldots\ldots\ldots\ldots\ldots\ldots\ldots\ldots\ldots\ldots \quad (10)$$

Simpson rule has been used to compute mean Nusselt number.

Numerical solution

A finite difference method (FDM) is used to descretize system of the partial differential equations (5 through 8) into algebraic equations system. The new algebra equations system will be solved using iterative under relaxation method, to give approximate values of the dependent variables at a number of discrete points called (grid points or nodes) in the computational domain. A grid was established by subdividing the computational domain in the R and ϕ directions with indexes i and j that are integers describing the number of radial grid lines from the inner cylinder and the number of angular grid lines from the top symmetry line respectively, as shown in Fig.(4.2).The spacing of the grid lines in the R-direction is uniform and given by ΔR and that of the grid lines in the ϕ-direction is also uniform and given by $\Delta\phi$. The number of the grid points will be [m × n] where (m) represents the number of gridlines in the R-direction and equals $[(1/\Delta R)+1]$ while (n) represents the number of gridlines in the ϕ-direction and equals $[(\pi/\Delta\phi)+1]$.

The partial differential equations (5)-(8) were finite-differenced using central difference schemes for all of the derivatives. In particular, let ξ represents $\Psi, \Omega, \text{or}\ \theta$, then

$$\frac{\partial \xi}{\partial R} = \frac{\xi_{i+1,j} - \xi_{i-1,j}}{2\Delta R}, \quad \frac{\partial \xi}{\partial \phi} = \frac{\xi_{i,j+1} - \xi_{i,j-1}}{2\Delta\phi}, \quad \frac{\partial^2 \xi}{\partial R^2} = \frac{\xi_{i+1,j} - 2\xi_{i,j} + \xi_{i-1,j}}{2\Delta R} \text{ and } \frac{\partial^2 \xi}{\partial \phi^2} = \frac{\xi_{i,j+1} - 2\xi_{i,j} + \xi_{i,j-1}}{2\Delta\phi}$$

Equations (5)-(8) were put in the form convenient for iterations with under relaxation method as;

$$\Psi^{\zeta+1}{}_{i,j} = \Psi^{\zeta}{}_{i,j} + \gamma_{\Psi}\left[h_1\Psi_{i+1,j} + h_2\Psi_{i-1,j} + h_3\left(\Psi_{i,j+1} + \Psi_{i,j-1}\right) + \frac{(\Delta R)^2}{h}\Omega_{i,j} - \Psi_{i,j}\right] \ldots\ldots (11)$$

$$\Omega^{\zeta+1}_{i,j} = \Omega^{\zeta}_{i,j} + \gamma_{\Omega}\left[h_4\Omega_{i+1,j} + h_5\Omega_{i-1,j} + h_6\Omega_{i,j+1} + h_7\Omega_{i,j-1} - \Omega_{i,j} + h_8\left(\theta_{i+1,j} - \theta_{i-1,j}\right) + h_9\left(\theta_{i,j+1} + \theta_{i,j-1}\right)\right] \quad \text{..... (12)}$$

$$\theta^{\zeta+1}_{i,j} = \theta^{\zeta}_{i,j} + \gamma_{\theta}\left[h_{10}\theta_{i+1,j} + h_{11}\theta_{i-1,j} + h_{12}\theta_{i,j+1} + h_{13}\theta_{i,j-1} - \theta_{i,j}\right] \quad \text{..... (13)}$$

Where h_1-h_{13} are parameters from the discretization;

$$h = 2\left[1 + \frac{1}{R^2}\left(\frac{\Delta R}{\Delta\phi}\right)\right] \qquad h_1 = \left(1 + \frac{\Delta R}{2R_i}\right)\Big/ h \qquad h_2 = \left(1 + \frac{\Delta R}{2R_i}\right)\Big/ h \qquad h_3 = \frac{1}{R_i^{\,2}}\left(\frac{\Delta R}{\Delta\phi}\right)^2\Big/ h$$

$$h_4 = \left(1 + \frac{\Delta R}{2R_i} - \frac{\Delta R}{2\,Pr}U_{i,j}\right)\Big/ h \quad h_5 = \left(1 - \frac{\Delta R}{2R_i} + \frac{\Delta R}{2\,Pr}U_{i,j}\right)\Big/ h \quad h_6 = \left(\frac{1}{R_i^{\,2}}\left(\frac{\Delta R}{\Delta\phi}\right)^2 - \frac{(\Delta R)^2}{2\,Pr\,R_i\Delta\phi}V_{i,j}\right)\Big/ h$$

$$h_7 = \left(\frac{1}{R_i^{\,2}}\left(\frac{\Delta R}{\Delta\phi}\right)^2 + \frac{(\Delta R)^2}{2\,Pr\,R_i\Delta\phi}V_{i,j}\right)\Big/ h \qquad h_8 = -Ra\frac{\Delta R}{2}\sin\phi_j / h \qquad h_9 = -Ra\frac{(\Delta R)^2}{2R_i\Delta\phi}\cos\phi_j / h$$

$$h_{10} = \left(1 + \frac{\Delta R}{2R_i} - \frac{\Delta R}{2}U_{i,j}\right)\Big/ h \qquad h_{11} = \left(1 - \frac{\Delta R}{2R_i} + \frac{\Delta R}{2}U_{i,j}\right)\Big/ h \qquad h_{12} = \left(\frac{1}{R_i^{\,2}}\left(\frac{\Delta R}{\Delta\phi}\right)^2 - \frac{(\Delta R)^2}{2R_i\Delta\phi}V_{i,j}\right)\Big/ h$$

$$h_{13} = \left(\frac{1}{R_i^{\,2}}\left(\frac{\Delta R}{\Delta\phi}\right)^2 + \frac{(\Delta R)^2}{2R_i\Delta\phi}V_{i,j}\right)\Big/ h$$

and $\gamma_{\Psi}, \gamma_{\Omega}$ and γ_{θ} are relaxation factors chosen from numerical experiments as:

$\gamma_{\Psi} = 0.8, \gamma_{\Omega} = 0.07$ & $\gamma_{\theta} = 0.7$.

These values of relaxation factors have been found to stabilize the computation procedure for Rayleigh number ranges (10^2 - 10^5) and increase considerably the rate of convergence. Number of iterations ranges (1000 - 1500) was enough to attain the required convergence. For the cases when Ra was increased to a critical value which was beyond the experimentally known laminar flow regime (Ra > 10^5) the solution diverged and the method becomes unstable.

During the computation, because of the slow rate of convergence for the stream function and vorticity compared with that of temperature, iteration was performed in weighted cyclic pattern as $(\Psi - \Omega - \Psi - \Omega - \theta)$.The convergence criteria needed for termination of the computation were preassigned as:

$(\Psi^{\zeta} - \Psi^{\zeta-1})/\Psi^{\zeta} \le 10^{-5}$, $(\theta^{\zeta} - \theta^{\zeta-1})/\theta^{\zeta} \le 10^{-5}$ and $(\Omega^{\zeta} - \Omega^{\zeta-1})/\Omega^{\zeta} \le 10^{-5}$

The calculations were performed on P4-computer using MATLAB-7 software.

EXPERIMENTAL STUDY

Experimental apparatus

The apparatus was designed and constructed specially for investigating the effect of Rayleigh number, diameter ratio and existing of annular fins on the natural convection heat transfer between two horizontal concentric cylinders of constant wall temperature under steady state conditions. The experimental apparatus is diagrammatically shown in Fig.(2). The test-section consists of a fixed (27mm) outside diameter, (5 mm) thick and (200 mm) long aluminium inner cylinder to which one of three different aluminium outer cylinders (200 mm) long, (4 mm) thick with 55,70 and 82 mm outside diameter were assembled to yield diameter ratios of 2, 2.6 and 3, respectively. The inner cylinder was made in two configurations, one in which the inner cylinder is being unfinned and another in which it being finned. Finned inner cylinder, shown in plate (1), is fixed to one of three different outer cylinders mentioned above, to give (fin height/gap width) of 0.286, 0.186 and 0.143.The test section is mounted on a wooden supporting-frame and stored horizontally with aid of a sprit level. The inner cylinder was heated by passing an alternative current through a 0.2-mm-dia, 5-m-length, 95-ohm nichrome wire wounded as spiral inside glass tube, (8 mm) in diameter and (190 mm) long. The heater, i.e. the glass tube and the nichrome wire, was mounted concentrically in the inner cylinder by two fictile pieces. The space between the glass tube and the inside surface of inner cylinder, also the space inside glass tube was filled by very fine sand to avoid generation of heat convection in it and to smooth any irregularities in the heat flux generated from the heater. The heater was connected in series to the power supply to ensure that incoming mains voltage is constant (220 V), and in parallel with the variac to adjust the heater input voltage as required. The voltage and current supplied to the heater were measured by digital voltmeter and ammeter of accuracy ± 0.05 volt and $\pm 5\times10^{-4}$ ampere. Temperatures on the inner and the outer cylinder surfaces were measured by thermocouples type T; several holes of (1.5 mm) in diameter were cut over along the surface of the cylinders to accommodate thermocouples .These holes are distributed as follows:

1. Six holes of (5 mm) deep on the surface of unfinned inner cylinder; two located at a distance of (30 mm) from the ends and four at the mid-plane 90° apart between them.
2. Six holes on the surface of finned inner cylinder, two of (5 mm) deep, located at a distance of (30 mm) from the ends and four of (9 mm) deep at the mid-plane 90° apart between them.
3. Four of (2 mm) deep on the outer cylinder surface; two located at a distance of (30 mm) from the ends and two at the mid-plane 180° apart between them.

The ends of the test-section were plugged with Teflon (an insulating material) pieces in order to minimize the axial end losses and to mount the inner cylinder concentrically inside the outer cylinder. The Teflon piece is a disc (85 mm) in diameter and (20 mm) thick, cut out radially in a (10 mm) thick to get a diameter equal to the inside diameter of the outer cylinder, and drilled axially in a distance of (10 mm) and diameter of (27 mm) to get a diameter equal to the outside diameter of the inner cylinder. A hole of (5 mm) in diameter was drilled axially in each Teflon piece to draw the heater terminals and the thermocouples lead outside the test-section. Two thermocouples (type T) were fixed on the inside and outside surface of each teflon piece to estimate conduction heat losses from the test section ends. The distance between these thermocouples was 14 mm. knowing the thermal conductivity of the teflon; the ends conduction losses could thus be calculated.

Experimental Procedure

Components of experimental rig were assembled in a windowless large room, free of air currents, to avoid occurrence of fluctuations in the room temperature.

The following Procedure steps have been followed in each test run:

- Mount the inner cylinder to appropriate outer cylinder to obtain a certain diameter ratio.
- Adjust the input power to the heater to obtain a certain Rayleigh number.
- Allow the test to run for a period until steady state condition was achieved. The steady state condition was considered to be achieved when the differences in the measured temperatures were not more than 0.2 °C over 30 min. In all the experiments, the steady state condition period was within 3–4 hours.
- After steady state condition has been established, the readings of all thermocouples, the input power and the ambient temperature were recorded.
- Repeat steps 2–4 for nine different Rayleigh numbers.
- Repeat steps 2–5 twice, once for case without fins and another for case with fins.
- Repeat steps 1–6 three times for different diameter ratio; 2.0, 2.6 and 3.0 .

RESULTS AND DISCUSSION

Experimental Results

Fig.(3) shows the variation of mean Nusselt number $\left(\overline{\mathrm{Nu}}\right)$ with Ra for different diameter ratios. This figure shows that for any diameter ratio, $\left(\overline{\mathrm{Nu}}\right)$ generally increases with increasing Rayleigh number.

Fig.(4) shows that ($\overline{\mathrm{Nu}}$) increases with increasing diameter ratio, and also shows that the curves of the different diameter ratios converge to each others as Ra decreases. This means that the effect of the diameter ratio on the heat transfer rate decreases with decreasing Ra.

Figs.(5) show the influence of attaching fins on inner cylinder surface on mean Nusselt number prediction . This figure indicates that there is a reduction in mean Nusselt number in the presence of fins as compared with case without fins. For the same value of Rayleigh number, reduction in Nusselt number may be ranged between (16.3% - 29.7%).The reason for this reduction is although the annular fins increase the surface area; they also resist the airflow. This resistance has been caused a decrease in heat transfer coefficient more than the increase in the surface area; as a consequence lower heat transfer rate was resulted.

Fig.(6) presents the effect of the ratio (fin height/gap width) on mean Nusselt number. At a lower value of fin height (14.3 percent of gap width) the mean Nusselt number seems to be relatively larger. One can conclude as the (fin height/gap width) increase the heat transfer coefficient decreases, this probably because of a larger (fin height/gap width) mean more obstruction for the fluid motion inside the cavity; consequently less convective heat transferred from inner cylinder.

Numerical Results

Effect of Rayleigh number

Left sides of Figs. (7) - (11) present streamlines at η=3.0 for different values of Rayleigh number (10^2-10^5). Fig.(7) depicts the streamlines at Rayleigh number of 10^2 which form a single ce11 rotates clockwise. This cell does not occupy uniformly the whole gap width. At this value of Rayleigh number the buoyancy force is very small to influence the temperature field and develop a fluid motion inside the annulus .A transition region exists for Rayleigh number between 10^3 and 10^4, Figs.(8-9). In this region, the flow remains in essentially the same pattern but become strong enough to influence the temperature field. As the Rayleigh number increases to 10^4 - 10^5, Figs.(9-10), A steady laminar boundary layer exists and the flow tends to occupy more uniformly the whole cavity and the center of circulation which defined as the point of the extremum of the stream function, begins to move higher up toward the upper symmetry line . The lower portion of the gap looks to be streamlines-free because this region is filled with a cold fluid and becomes stagnant. It is stagnant because the viscosity forces overcome the buoyancy forces and inhibit the fluid motion through it.

Right sides of Figs. (7) - (11) show the isotherms for diameter ratio of 3.0 with different values of Rayleigh numbers (10^2-10^5). For smaller Rayleigh number (10^2), the velocity is too small to affect the temperature distribution which remains essentially as in pure conduction. This makes the convection term in Eq.(8) vanish, therefore Eq.(8) can be approximated by $\left(\nabla^2\theta = 0\right)$, so the isotherms are almost uniformly concentric as shown in Fig.(7). For Rayleigh number of Ra=10^3, the isotherms indicates that the conduction stills the dominant heat transfer mechanism in the cavity. In other words, buoyancy forces are not strong enough to trigger significant convection. As the Rayleigh numbers increase to 10^4, convection becomes dominant mode of heat transfer, and stronger recirculation for the fluid will be occurred making the outer fluid layer warmer than the inner one causing at the core so called temperature reversal phenomenon. This phenomenon is depicted by isotherms of Figs.(9),(10) and (11). It is noticed in Figs.(10) and (11) that the isotherms are spaced more closely against the bottom of the inner cylinder and top of the outer cylinder, where the inner and outer cylinder thermal boundary layers are, respectively, thinnest. This mean maximum heat transfer from inner cylinder is from its lower portion while maximum heat transfer to outer cylinder is from upper portion; therefore heat is being essentially convected from lower portion of the inner cylinder to the top of the outer cylinder. In comparison of isotherms in Figs.(10) and (11) one can conclude as Rayleigh number increases isotherms at the lower portion of the inner cylinder and at the upper portion of the outer cylinder are further compressed.

Fig.(12) illustrates the distribution of local Nusselt number along the circumstance of the inner cylinder for the cases of Rayleigh number of 10^3, 10^4, 5×10^4 &10^5 .The local Nusselt number has an increasing trend from the top (0°-position) to the bottom (180°-position), where the highest values are reached. There are three regions can be distinguished in Fig.(12):

First region $\left(140^\circ < \phi < 180^\circ\right)$, in this region local Nusselt number is relatively constant since the inner boundary layer is of relative uniform thickness (see isotherms), and gives a little variation in local Nusselt distribution.

Second region $\left(10^\circ < \phi < 140^\circ\right)$, in this region local Nusselt number looses the uniformity and a large gradient in its distribution can be observed, this because the

inner boundary layer get thicker in this region since heat removal by fluid decreases as the fluid scends up

Third region $(0^o < \phi < 10^o)$, here values of local Nusselt number approach to its minimum values, this due to formation of plume in this region. formation of the plume occurs where the two convective currents coming from the two annulus halves, impinging with each other and moving together upward without mixing, leaving a relatively stagnant region under impinging point. This behavior is roughly similar for most of Rayleigh numbers.

Fig.(13) illustrate the relation between mean Nusselt number and Rayleigh number at η = 3.0. $\overline{Nu}$ is nearly constant at (10^2 <Ra< 10^3) because of the predominance of conduction mode on heat transfer process. Beyond Ra of 5×10^3 convection become predominant mechanism and $\overline{Nu}$ begins to largely increase.

Effect of diameter ratio

The left side of Fig.(14) illustrates the flow patterns moving inside the gap. Although the flow pattern does not change significantly, the center of rotation moves towards the top with increasing diameter ratio. That mean as the diameter ratio increases the flow become stronger.

Fig.(15) illustrates the effect of increasing η on local Nusselt number distribution around the inner cylinder circumference. It can be seen from this figure that for all the cases decreasing the diameter ratio decreases the local Nusselt number since the resistance to the circulation motion of the convection cells increases as η decreases and this leads to slower replacement of the hot air adjacent to the inner annulus surface by the cold air adjacent to the annulus outer surface and this results in a decrease of the heat transfer rate.

Comparison of present numerical and experimental results

		$\overline{Nu}$		
		Exp.	Num.	% Dev.
η =2.0	Ra = 1.81×10^3	1.823	1.653	9.3
η =2.0	Ra = 5.76×10^3	2.656	2.406	10.4
η =2.6	Ra = 5.40×10^3	2.933	2.766	5.6
η =2.6	Ra = 1.76×10^4	4.086	3.813	6.6
η =3.0	Ra = 1.14×10^4	3.662	3.796	3.6
η =3.0	Ra = 4.03×10^4	4.880	5.184	6.2

%Dev. = ((exp. value – num. value) / exp. value) × 100%

CONCLUSIONS

Natural convection heat transfer between two horizontal concentric cylinders with and without annular fins attached to the inner cylinder was investigated numerically (for case without fins only) and experimentally (for both cases) under steady-state conditions. The experimental results showed that annular fins of (No. of fins/cm) of 1.25 and (fin height/gap width) of 0.143, 0.186 and 0.286 have negative effect on heat

transfer results and cause a reduction in mean Nusselt number within (16.3 – 29.7) percent of that for the case without fins at the same Rayleigh number, and higher (fin height/gap width) has some blocking effect on fluid motion inside the cavity, therefore If there is a tendency toward reducing heat transfer rate between the horizontal concentric cylinders, it is better to use high (fin height/gap width). The numerical results showed that the heat is essentially transferred from the bottom of the inner cylinder to the top of the outer cylinder owing to the strong convective motion due to the buoyancy at these positions and decreasing of the diameter ratio increase the resistances to the circulation motion which leads to slower replacement of the hot air adjacent to the inner cylinder by the cold air adjacent to the outer cylinder and this results in a decrease of the heat transfer rate.

REFERENCES

- **Kuehn, T. H. and Goldstein, R. J.,** "An Experimental and Theoretical Study of Natural Convection in the Annulus between Horizontal Concentric Cylinders", J. Fluid Mech., Vol. 74, Part 4, Pp. 695-719, 1976.
- **Hessami, M. A., Pollard, A. and Rowe, R.W.,** "A Study of Free Convective Heat Transfer in A Horizontal Annulus with A Large Radii Ratio", ASME, J. Heat Transfer, Vol. 107, Pp. 603-610, 1985
- **Nada, S. A.,** "Experimental Investigation of Natural Convection Heat Transfer In Horizontal and Inclined Annular Fluid Layers", Int. J. Heat Mass Transfer, Vol. 50, 2007.
- **Tsui, Y. T. and Tremblay, B.,** "Transient Natural Convection Heat Transfer in the Annulus between Concentric Horizontal Cylinder with Isothermal Surfaces", Int. J. Heat Mass Transfer, Vol. 27, No. 1, Pp. 103-111, 1984.
- **Mahony, D.N., Kumar, R., and Bishop, E. H.,** "Numerical Investigation of Variable Property Effects on Laminar Natural Convection of Gases between Two Horizontal Concentric Cylinders", ASME, J. Heat Transfer, Vol. 108, Pp. 783-789, November 1986.
- **Kumar, R.,** "Study of Natural Convection in Horizontal Annuli", Int. J. Heat Mass Transfer, Vol. 31, No.6, Pp. 1137-1148, 1988.
- **Patankar, S.V. and Chai, J.C.,** "Laminar Natural Convection in Internally Finned Horizontal Annulus", Numerical Heat Transfer, Vol. 24, Pp. 67–87, 1993.
- **Rahnam, M. and Farhadi, M.,** "Effect of Radial Fins on Two-Dimensional Turbulent Natural Convection in A Horizontal Annulus", Int. J. Thermal Sciences, Vol. 43, Pp. 255-264, 2004.

- **Padilla, E. L. M., Campregher, R. And Silveira-Neto, A.,** "Numerical Analysis of Natural Convection in Horizontal Annuli at Low and Moderate Rayleigh Numbers", Thermal Engineering, Vol. 5, No.4, Pp. 58-65, 2006.
- **Teertstra, P. And Yovanovich, M. M.,** "Comprehensive Review of Natural Convection in Horizontal Circular Annuli", University Of Waterloo, 1998.
- **Roach. , P.J.** "Computational Fluid Dynamics", Hermosa, Albuquerque, New Mexico, 1985.
- **الشمري،منار صالح، " دراسة نظرية و عملية لانتقال الحرارة بالحمل الحر خلال فجوة حلقية مائلة "، أطروحة ماجستير، جامعة تكريت 2005.**

NOMENCLATURE

D	diameter
g	acceleration
m	number of gridlines in R-direction
n	number of gridlines in ϕ-direction
Nu	local Nusselt number
$\overline{Nu}$	mean Nusselt number
p	pressure
Pr	Prandtl number
Ra	Rayleigh number base on gap width
Ra_{Di}	Rayleigh number based on annulus inner diameter
r	radial coordinate
R	dimensionless radial coordinate
T	temperature
u,v	velocity components in *R*-, ϕ-directions
U,V	dimensionless velocity components in *R*-, ϕ-directions

Greek symbols

α	thermal diffusivity
β	thermal expansion coefficient
δ	gap width
Δ	laplacian in polar coordinates
η	diameter ratio
ν	kinematic viscosity
ω	vorticity
Ω	dimensionless vorticity
ψ	stream-function
Ψ	dimensionless stream-function
ρ	density
θ	dimensionless temperature

Subscripts

i	radial mesh point
j	angular mesh point
i	inner cylinder
^{o}	degree
o	outer cylinder

Superscripts

ζ	current iteration number
$\zeta+1$	next iteration number
$-$	mean

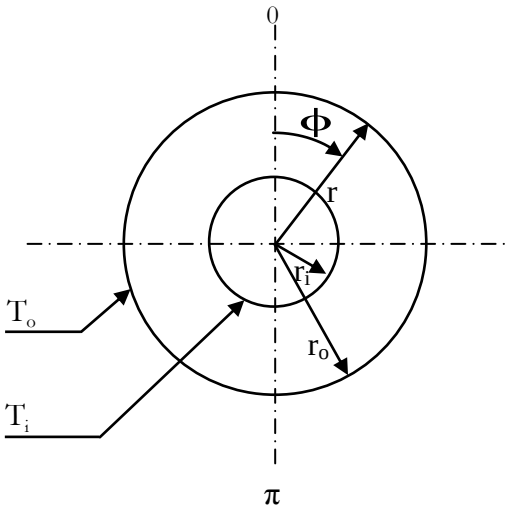

Fig.(1) Physical and Coordinate system

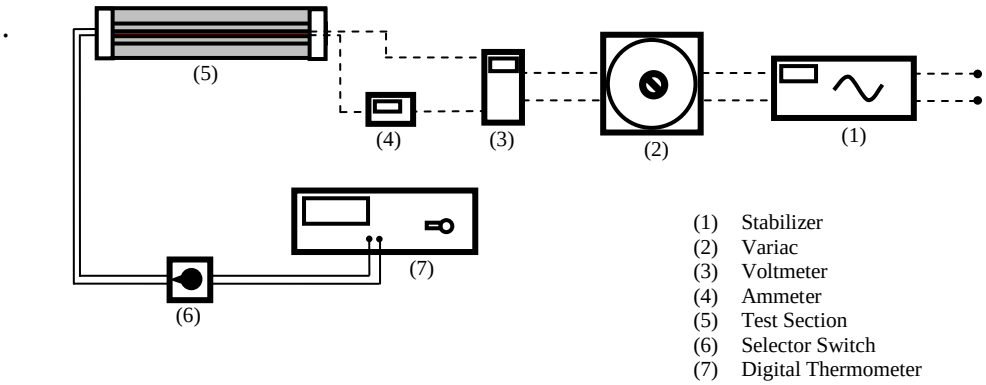

Fig. (2) Schematic diagram of experimental apparatus

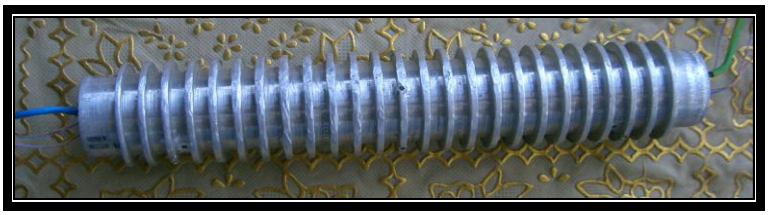

Plate (1) Inner finned cylinder

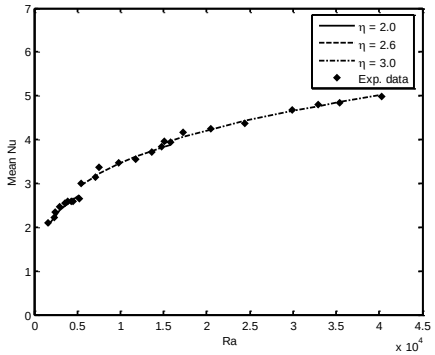

Fig (3) Mean Nusselt number as a function of Rayleigh number

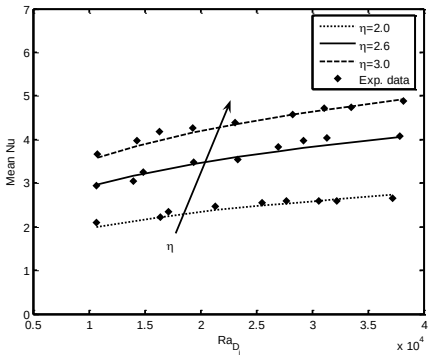

Fig (4) Effect of diameter ratio on mean Nusselt number predictions

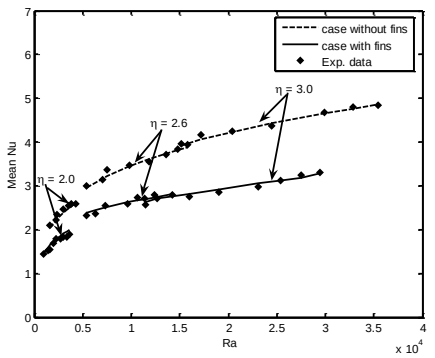

Fig (5) Effect of annular fins on mean Nusselt number predictions

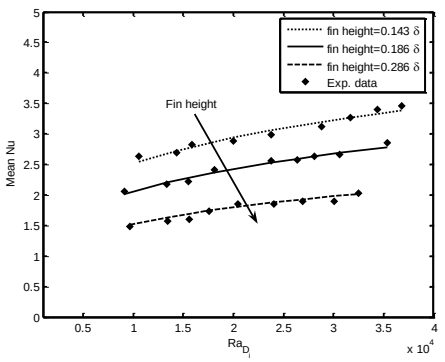

Fig (6) Effect of (fin height/gap width) on mean Nusselt number predictions

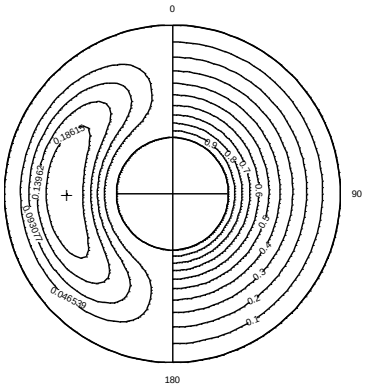

Fig (7) Isotherms and streamlines at η=3.0 , Ra=10^2

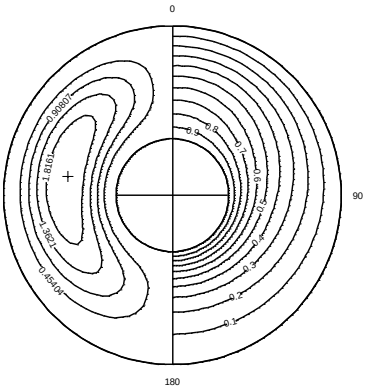

Fig (8) Isotherms and streamlines at η=3.0 , Ra=10^3

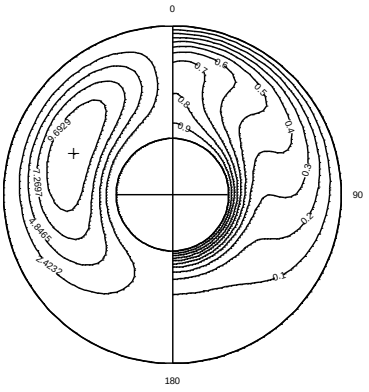

Fig (9) Isotherms and streamlines at η=3.0 , Ra=10^4

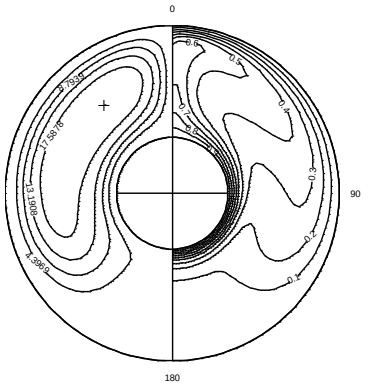

Fig (10) Isotherms and streamlines at η=3.0 , Ra=5×10^5

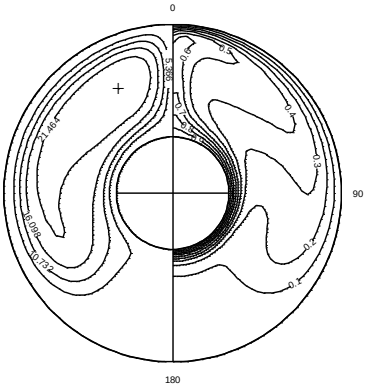

Fig (11) Isotherms and streamlines at η=3.0, Ra=10^5

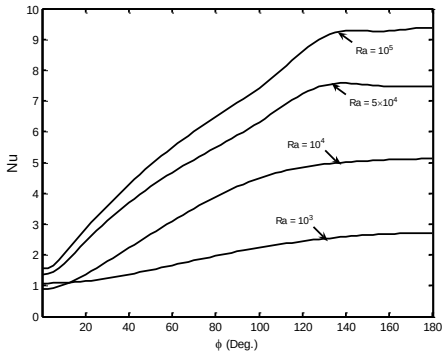

Fig (12) local Nusselt number distribution around the circumference of the inner cylinder at η=3.0 and different Rayleigh numbers

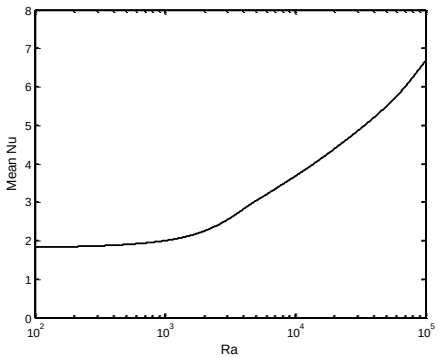

Fig (5.27) Mean Nusselt number versus Rayleigh number at η=3.0

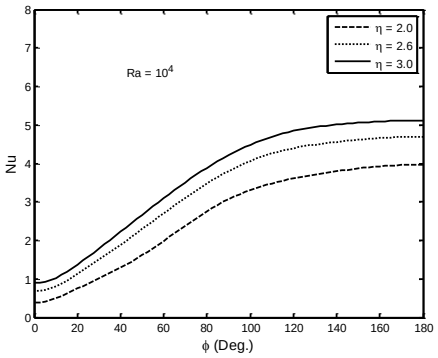

Fig (14) local Nusselt number at η=2.0, 2.6 , 3.0 and Ra=10^4

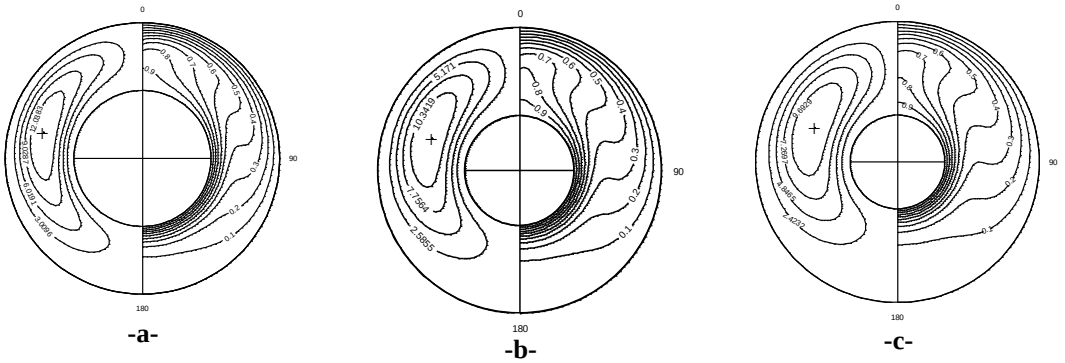

-a- **-b-** **-c-**

Fig (15) Streamlines and isotherms for Ra=10^4 at: a- η=2.0, b- η=2.6 and c- η=3.0